THE JOURNAL OF PHYSICAL CHEMISTRY B

Article

pubs.acs.org/JPCB

Multicompartmental Hollow Micelles Formed by Linear ABC Triblock Copolymers in Aqueous Medium

Shaoliang Lin,[†] Wenjie Zhu,[†] Xiaohua He,*[,‡] Yaohui Xing,[†] Liyuan Liang,[‡] Tao Chen,[†] and Jiaping Lin*[,†]

[†]Shanghai Key Laboratory of Advanced Polymeric Materials, Key Laboratory for Ultrafine Materials of Ministry of Education, School of Materials Science and Engineering, East China University of Science and Technology, Shanghai 200237, China

[‡]Department of Chemistry, East China Normal University, Shanghai 200241, China

ABSTRACT: Self-assembly behavior of an ABC triblock copolymer, poly(ethylene glycol)-*b*-polystyrene-*b*-poly(ε-caprolactone) (PEG-*b*-PS-*b*-PCL), in aqueous media is presented. The formed micelle structures were analyzed by using transmission electron microscopy, scanning electron microscopy, and laser light scattering. Various fascinating multicompartmental aggregates, including multilamellar vesicles, cylinder-containing vesicles, entrapped vesicles, and porous large compound micelles, were prepared from four copolymers with various block lengths of PEG and PS. The phase separation of hydrophobic PS and PCL blocks, as well as the hydrophilic/hydrophobic balance, plays a crucial role on the self-assembly behaviors. The mechanism regarding the formation of these fascinating aggregates is also suggested.

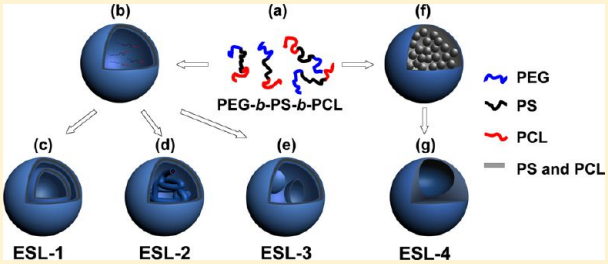

1. INTRODUCTION

Block copolymers, which consist of two or more different covalently linked polymers, are a well-known and developed class of macromolecules that can self-assemble into various nanostructures in aqueous media or mixed organic solvents.[1−4] The formed nanostructures ranging from spheres to cylinders, vesicles, lamellae, and tubules to large compound micelles have attracted significant attention for potential applications in the dispersant technology, nanomaterial synthesis, the targeted delivery and controlled release of drugs.[5−12] Recently, hollow structures, such as vesicles, porous spheres, and tubules, have become a hotspot due to their unique architectures and extraordinary properties.[13,14] Plenty of methods were used to obtain such aggregates, including tuning the copolymer composition and architecture, the preparation conditions, and other particular methods.[15−18]

For AB- and ABA-type block copolymers, the self-assembly behaviors are widely studied and the factors governing self-assembly are well understood.[19] However, the self-assembly of linear ABC triblock copolymers have lately been investigated thanks to the advances in polymer synthesis technologies.[20−23] When a third gradient was added, the micellization behavior becomes complex. This is caused by the effects of block/selective solvent combinations, the possible arrangements of block sequence (ABC, ACB, BAC, and miktoarm star ABC), and also the arrangements of chains in the micelles.[24−27]

Up to now, the possibilities of self-assembly of ABC triblock copolymers in a selective solvent still remain quite unexplored, especially for the case that two of the three ABC segments are insoluble in the solvent.[28−30] If the core-forming blocks are incompatible, they may segregate into different phases within the core of the micelle to generate multicompartment micelles, which are characterized by such segregated incompatible subdomains.[30−32] The multicompartment core, such as "spheres in spheres" (core−shell−corona model, onion like) or "spheres on spheres" (raspberry like), has widely been explored.[30,33] For instance, Lodge et al. prepared oblate ellipsoid micelles with a core−shell−corona structure by using selective fluorinated poly(ethylene oxide)-*b*-poly-(styrene)-*b*-1,2-poly(butadiene) block copolymers. The elongation of the micelles is ascribed to the strong incompatibility of the poly(styrene) and fluorinated poly(butadiene) blocks.[33] Kubowicz et al. have studied the aqueous self-assembly of an ABC linear triblock copolymer, poly(4-methyl-4-(4-vinylbenzyl) morpholin-4-ium chloride)-*b*-polystryrene-*b*- poly-(pertafluorophenyl 4-vinylbenzyl ether) (PVBM-*b*-PS-*b*-PVBFP). A raspberry-like morphology of micelle core containing insoluble PS and PVBFP blocks is found, where many small PVBFP-rich domains coexist with a continuous hydrocarbon domain of PS and PVBFP.[30]

On the other hand, if the hydrophilic/hydrophobic volume ratio is rather low, the morphology region will change from spherical micelles to large compound micelles or vesicles. In these cases for an ABC block copolymer, the phase separation in the aggregates would lead to a more complex and fascinating self-assembly behavior.[17] In a recent report, Grason et al. found that poly(isoprene-*b*-styrene-*b*-2-vinyl pyridine) (PI-*b*-PS-*b*-P2VP) triblock copolymer can form vesicles within the nanopores of an anodic aluminum oxide membrane. The microphase separation of PS and PI blocks in the hydrophobic

Received: December 30, 2012
Revised: February 4, 2013
Published: February 6, 2013

   dx.doi.org/10.1021/jp312858e | *J. Phys. Chem. B* 2013, 117, 2586−2593

membranes causes the formation of a unique meshlike morphology.[17] However, works with respect to this field are still very limited.

In this study, the self-assembly behavior of an amphiphilic ABC triblock copolymer, poly(ethylene glycol)-*b*-polystyrene-*b*-poly(ε-caprolactone) (PEG-*b*-PS-*b*-PCL), containing two incompatible hydrophobic blocks of PS and PCL, was studied in aqueous media. The hydrophilic PEG is of special interest not only due to its innocuity and biocompatibility, but also its unique properties of low protein adsorption and low cell adhesion. The semicrystalline PCL is one of the most commonly studied biodegradable aliphatic polyester.[34−38] The PS has been widely used as a hydrophobic segment of amphiphilic copolymer for self-assembly researches.[39] The combination of the three blocks leads to an informative structure of PEG-*b*-PS-*b*-PCL triblock copolymer, and extensive applications of its self-assemble system. The multicompartment morphologies within the aggregate core were obtained by tailoring the molecular architecture. The possible mechanism of aggregation formation is also suggested.

2. EXPERIMENTAL SECTION

2.1. Materials. ε-Caprolactone was purchased from Aldrich and distilled over CaH_2 under vacuum before use. Styrene was purchased from Merck and pretreated by passing through a basic alumina column to remove the inhibitor and followed by distillation over CaH_2 under vacuum. PEG was purchased from Aldrich (M_n = 2000). The purifications of CuBr, toluene, and other solvents and the preparation of macroinitiator PEG-Br were done according to published procedures.[40,41] Sodium azide (Acros, 99%), PMDETA (Aldrich, 99%), propargyl alcohol (Aldrich, 99%), 4-(dimethylamino)pyridine (DMAP) (Acros, 99%), 2-bromo-2-methylpropionyl bromide (Acros, 98%) were used without further purification. Stannous octanoate ($Sn(Oct)_2$), tetrahydrofuran (THF), and *N*,*N*-dimethylformamide (DMF) were of analytical grade and used without further purification.

2.2. Synthesis of PEG-*b*-PS-*b*-PCL Triblock Copolymers. PEG-*b*-PS-*b*-PCL (ESL) triblock copolymers were prepared by the method presented detailedly in the ref 41. First, bromine-terminated diblock copolymers PEG-*b*-PS-Br were prepared by ATRP of styrene and converted into azido-terminated PEG-*b*-PS-N_3 diblock copolymers. Propargyl-terminated PCL was prepared by ROP of ε-caprolactone in toluene with $Sn(Oct)_2$ as a catalyst and propargyl alcohol as an initiator. Then PEG-*b*-PS_2-N_3, propargyl-terminated PCL, CuBr, and DMF were added into a flask, and purged with N_2 for 15 min, followed by the addition of PMDETA. The mixture was stirred overnight at room temperature and then was precipitated into methanol. The samples were purified by reprecipitating three times from THF into methanol and dried at room temperature in a vacuum oven for 48 h. Four triblock copolymers denoted ESL-1, ESL-2, ESL-3, and ESL-4 were synthesized. The molecular weights M_n and polydispersity M_w/M_n were measured by gel permeation chromatography (GPC) (Waters 150 °C) equipped with three Waters Styragel columns (10^3, 10^4, and 10^5 Å) and an RI detector using THF as an eluent at 35 °C. The column system was calibrated by a set of monodispersed standard polystyrenes. The characteristics of these four samples are shown in Table 1.

2.3. Preparation of ESL Aggregate Solutions. To prepare the aggregate solutions, the obtained ESL samples were first dissolved in the common solvent of THF (or DMF).

Table 1. Characteristics of the PEO-*b*-PS-*b*-PCL Triblock Copolymers

sample	M_n[a] (10^4 g/mol)	M_w/M_n[a]	$M_{n\text{-PEG}}$[a] (10^3 g/mol)	$M_{n\text{-PCL}}$[a] (10^3 g/mol)
ESL-1	1.62	1.10	3.10	7.10
ESL-2	1.96	1.09	3.10	7.10
ESL-3	3.30	1.13	7.90	7.10
ESL-4	4.70	1.16	7.90	7.10

[a]Molecular weights of triblock copolymers, PEG and PCL precursors determined by GPC in THF. The molecular weights and molecular weight distributions were calculated by reference to a PS standard calibration curve.

The initial polymer concentration was maintained at 0.1 g/L. Then 10 mL of deionized water, a selective solvent for PEG, was dropwise added to 10 mL of polymer solution at a rate of 2 mL per minute with vigorous stirring, and finally dialyzing the resulting solution against water. The aggregate solutions were diluted with deionized water to 0.01 g/L and stabilized for 48 h before the measurements. All of the sample preparation processes were performed under 20 °C.

2.4. Characterization. *Transmission Electron Microscopy (TEM).* The morphologies of the micelles were examined by TEM (JEM-2100F). Drops of micelle solution were placed on a carbon film coated copper grid, and then were dried at room temperature. Before the observations, the sample was stained by phosphotungstic acid aqueous solution (0.5 wt %). The TEM bright filed imaging was performed with 200 kV accelerating voltage.

Scanning Electron Microscopy (SEM). The morphologies of the aggregates were also observed by SEM (JSM 6460, JEOL) operated at an accelerating voltage of 20 kV. The samples were prepared by placing drops of solution on a copper grid coated with carbon film and then drying them at room temperature. Before the observations, the samples were sputtered by carbon.

Laser Light Scattering (LLS). Laser light scattering was measured by a LLS spectrometer (ALV/CGS-5022) equipped with an ALV-High QE APD detector and an ALV-5000 digital correlator using a He−Ne laser (the wavelength λ = 632.8 nm) as the light source. All the measurements were carried out at 25 °C. In static light scattering (SLS) measurement, the angular dependence of the excess absolute time-average scattered intensity; i.e., Rayleigh ratio $R(q)$ of the dilute dispersion leads to the root-mean-square z-average radius of gyration $\langle R_g \rangle$, where $q = 4\pi n \sin(\theta/2)/\lambda$ is the scattering vector as a function of scattering angle θ, n is the refractive index of the solution, and λ is the wavelength of the incident beam. In dynamic light scattering (DLS) measurement, the Laplace inversion of each measured intensity−intensity time correlation function $G(2)(t,q)$ in the self-beating mode can result in a line width distribution $G(\Gamma)$. The translational diffusion coefficient D calculated from the decay time, Γ, by the slope of the Γ vs q^2 plot, can lead to hydrodynamic radius $\langle R_h \rangle$ by the Stokes−Einstein equation $R_h = k_B T/(6\pi\eta D)$, where k_B, T, and η are the Boltzmann constant, the absolute temperature, and the solvent viscosity, respectively.

3. RESULTS AND DISCUSSION

3.1. Morphology of Aggregates Observed by TEM and SEM. Because of the amphiphilic characteristics, ESL triblock copolymers in the selective solvent can self-assemble into aggregates, where the hydrophobic PS and PCL blocks

dx.doi.org/10.1021/jp312858e | J. Phys. Chem. B 2013, 117, 2586−2593

tend to form the core of the aggregates and the hydrophilic block PEG form the shell to stabilize the aggregates. As reported, crystallization of one component can drive phase separation because it can cause release of noncrystallizable blocks.[42] Due to the incompatibility of hydrophobic blocks of PS and PCL, the phase separation of the two blocks occurs and the multicompartment morphology within the aggregates can be expected.[43−46]

The structures of the various aggregates formed by ESLs are observed by TEM. Figure 1 shows the TEM images of the

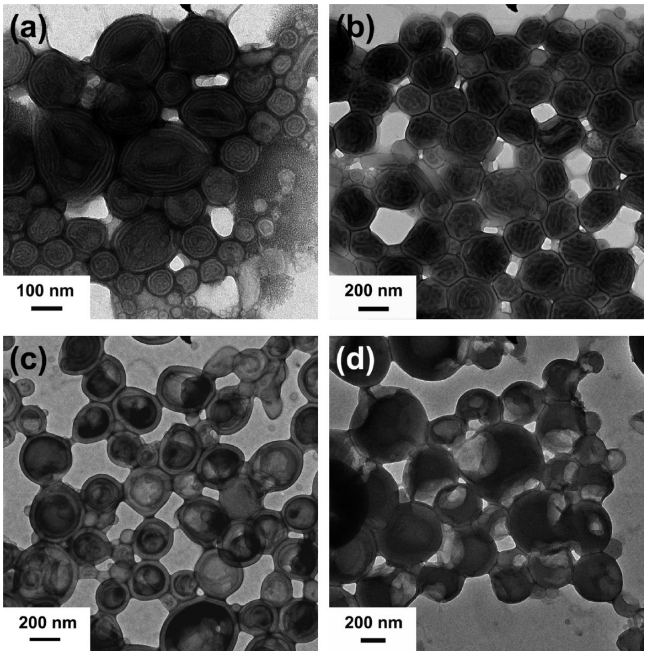

Figure 1. TEM images of the multicompartment micelles formed by various PEO-*b*-PS-*b*-PCL samples: (a) ESL-1, (b) ESL-2, (c) ESL-3, and (d) ESL-4.

resulting aggregates formed by the four copolymers. The morphologies of the self-assembled aggregates were found to be strongly dependent upon the component of the copolymers. In the case of ELS-1, multilamellar vesicles can be observed as shown in Figure 1a. The diameter distribution is relatively broad with a range of 50−400 nm. The multilamellar vesicles consist of up to six layers with a wall thickness about 12 nm. It was also observed that some large aggregates are obviously collapsed, which suggests that multilamellar vesicles have hollow structures.

Figure 1b shows the morphology of aggregates formed by ELS-2, which has the same PEG and PCL blocks but longer PS blocks as compared to ELS-1. A novel large compound micelle can be obtained, where the outer shell is a large vesicle and a lot of cylinders inside. The vesicles have a diameter of about 220 nm and a wall thickness of about 16 nm. It is worth noting that shells of the vesicles have a lower contrast compared with the interior area, which indicates that the crimps are solid cylinders rather than channels around the shell. The cylinders have a uniform thickness of about 15 nm and twist into concentric toris in most cases.

In the present instance, it is well-known that incompatibility between semicrystalline PCL and amorphous PS can bring about phase separation in confined geometries include lamella, cylinders, and spheres.[47−49] Because PCL is a semicrystalline block and PS possesses a relative high T_g value, the terpolymers must have a low mobility in the THF/H_2O mixed solution. As speculated by Eisenberg et al., multilamellar vesicles are similar to the formation of the lamellar phase in bulk. In many cases, copolymers which form multilamellar vesicles have a composition that would yield the lamellar phase in bulk.[50] ESL-1 has a molecular weight ratio of about 6:7 (PS:PCL), which is in the lamella region for most bulk systems. Hence, the multilamellar vesicle shown in Figure 1a exhibits a specific type of lamella structure, performs on limited space, and is closed to avoid the thermodynamic penalty of end-cap or rim formation. However, for the sample ESL-2 which has a high molecular weight of PS, the molecular weight ratio of PS and PCL is about 10:7. Such a molecular structure of PS and PCL blocks may drive them to phase separate to form cylindrical structure, where the short PCL blocks aggregate to form the core surrounded by longer PS blocks. As a result, the cylinder-containing vesicles formed by ESL-2 can be obtained as illustrated in Figure 1b.

TEM images of another group ESL-3 and ESL-4, which have longer PEG block and PS block with an identical PCL block as compared to ESL-1 and ESL-2, are shown in Figure 1, c and d. Most vesicles with a diameter ranging from 100 to 300 nm and a wall thickness of about 26 nm are formed by ESL-3 (Figure 1c). The thickness is larger than that of multilamellar vesicles formed by ESL-1 due to the larger hydrophobic components of PS block. The image in Figure 1c also exhibits large vesicles encapsulating small vesicles, similar to the entrapped vesicles.[50−52] This phenomenon may be caused by the lower mobility of the high molecular weight system. When THF was removed from large vesicles and water diffused in, some copolymers are entrapped in the vesicles and further self-assemble into smaller vesicles inside.

Figure 1d shows unusual porous spheres which commonly consist of two "caves" formed by ESL-4. Most of the aggregates have diameters between 300 and 600 nm. The dimension of such a structure's solid part is much larger than the ESL-4 extended chain length. Similar peculiar structures have also been reported by other groups and were called bowllike structures. Eisenberg et al. first reported the bowllike structures prepared from 5-(*N*,*N*,*N*-diethylmethylammonium)isoprene and styrene block copolymers (PAI-*b*-PS-*b*-PAI),[53] and then in another system observed such structures through the self-assembly of poly(styrene-*co*-methacrylic acid) [P(St-*co*-MAA)].[54] Jiang et al. also observed bowllike structures from the self-assembly of the rigid polyimide with two carboxyl ends.[55] The formation of the aggregates might involve three steps. First, when water is dropped into the copolymer solution, large compound micelle (LCM) is formed, which is composed of many inverse micelles inside and an exterior PEG corona. Second, when more water is added and THF diffuses outward, interior bubbles form because of shrinkage of inverse micelles inside and hardening of the shell. At last, the bubbles coalesce and try to break through the thinnest part of the aggregates until the aggregates are freezing. If the freezing of the shell is more rapid than the diffusion of the bubbles, the bubbles would be entrapped and form caves in the large component micelles.

We also employ SEM to confirm the aggregation structures formed by ESL samples (Figure 2). As shown in Figure 2a, the hollow structure of the multilamellar vesicles is further confirmed by the broken shells. Although the aggregates formed by ESL-2 are also hollow as judged from some caves, they do not collapse drastically due to the support of the

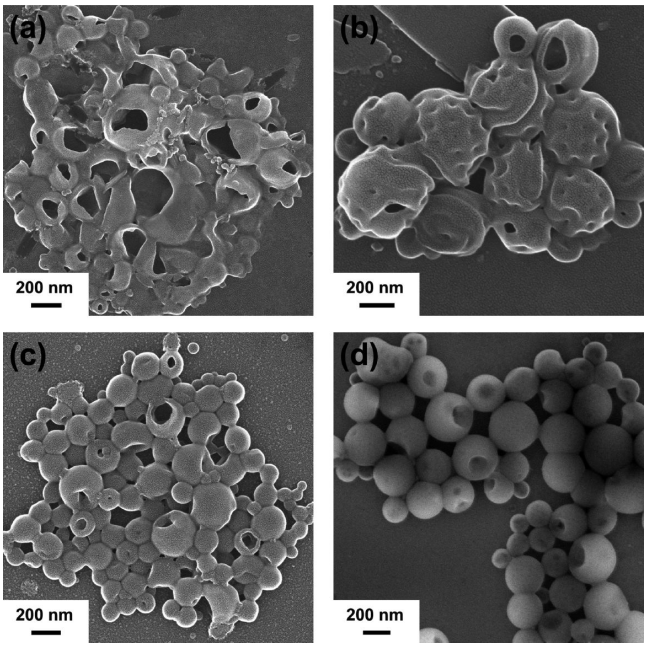

Figure 2. SEM images of the multicompartment micelles formed by various PEO-*b*-PS-*b*-PCL samples: (a) ESL-1, (b) ESL-2, (c) ESL-3, and (d) ESL-4.

cylinders. The patterning surfaces distinctly reflect the interior structures (Figure 2b). These characters further confirm the unique cylinder-in-vesicle structure. The aggregates formed by ESL-3 are also partially collapsed (Figure 2c), which correspond to the entrapped vesicles. It is clear seen from Figure 3d that the spheres of ESL-4 do not have distinct deformation in the SEM sample preparation showing the solid structure and most of them contain two "caves". Such a 3D special structures are in consistent with the TEM result as illustrated in Figure 1d.

3.2. Aggregate Size and Structure Studied by LLS.

To get the information of the aggregates in aqueous solution, we further analyzed the formed aggregates for these copolymers by combining DLS and SLS measurements. DLS was used to assess the average hydrodynamic sizes of the formed aggregates. Figure 3a exhibits the CONTIN plots for ESL-2 aggregates at a scattering angle of 90°. The value of R_h is much larger than that of the individual chain, showing a clear self-assembly of ESL copolymers. The corresponding polydispersities (PDI) calculated via cumulant analysis for all the ESL aggregates are shown in Table 2. The values of PDI are around 0.2, implying that these self-assembled ESL nanostructures are well-defined with a relatively uniform particle size.

Table 2. Solution Characteristics of the PEO-*b*-PS-*b*-PCL Copolymers in Aqueous Media with THF as Common Solvent

sample	$\langle R_h \rangle$ (nm)	PDI[a]	$\langle R_g \rangle$ (nm)	$\langle R_g \rangle / \langle R_h \rangle$
ESL-1	133.1	0.138	135.3	1.02
ESL-2	168.2	0.081	134.4	0.799
ESL-3	173.0	0.137	141.5	0.818
ESL-4	266.9	0.213	231.1	0.866

[a]Deviation determined by cumulant analysis at the scattering angle of 90°.

The hydrodynamic radium of the aggregates can be obtained from the plot of decay rate, Γ, against q^2, where $\Gamma = 1/t$, and t is the decay time. The plot for the ESL-2 aggregates as an example is shown in Figure 3b. The linearity of the decay rate plots and the lack of an intercept indicate a pure translational diffusion, which is typical of spherical particles. According to the equation $\Gamma = Dq^2$, the slope of the plot can lead to a D value. Based on the Stokes–Einstein equation, $\langle R_h \rangle$ of aggregates in aqueous solution can be calculated. The average hydrodynamic radium $\langle R_h \rangle$ can be obtained as 168 nm. The results of all samples are showed in Table 2. From the results, we can see that the $\langle R_h \rangle$ value increases with the increase of molecular weights at a fixed PEO chain length. This is because the polymers with a higher molecular weight have a higher hydrophobicity, which lead to a larger aggregation number to stabilize the aggregates. The $\langle R_h \rangle$ values of ESLs are a little larger than the respective TEM and SEM images. This is caused by the shrinkage of the hollow structures in the dry state.

Figure 4 shows a typical Guinier plot of the ESL-2 aggregates in water at 20 °C, which incorporates the angular dependence

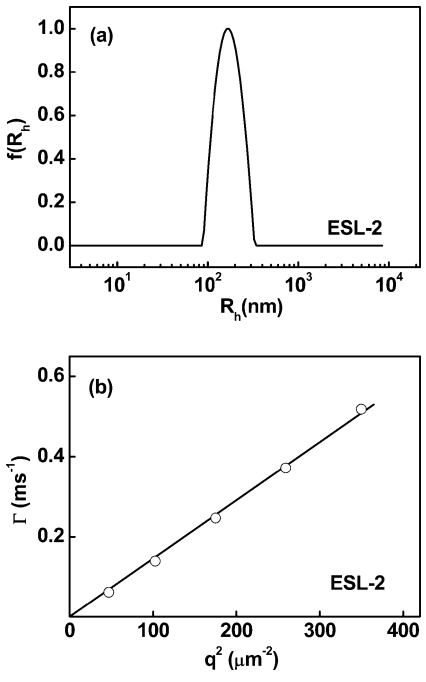

Figure 3. (a) Typical hydrodynamic radius distribution $f(R_h)$ of ESL-2 micelles. (b) Plot of decay rate Γ against q^2 for ESL-2 micelle solution.

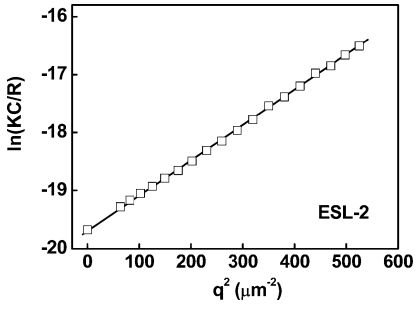

Figure 4. A typical plot for the angular dependence of the ln(KC/R) for ESL-2 micelle solution.

dx.doi.org/10.1021/jp312858e | J. Phys. Chem. B 2013, 117, 2586–2593

of Rayleigh ratio $R(q)$. The slope of $\ln[KC/R(q)]$ vs q^2 can lead to R_g, and further to the ratio of $\langle R_g \rangle$ to $\langle R_h \rangle$, which is sensitive to the particle shape.[56−58] $\langle R_h \rangle$ is defined as the radius of a hard sphere with the same translational diffusion coefficient and the same condition, while $\langle R_g \rangle$ reflects the density distribution of the chain in real physical space. The $\langle R_g \rangle / \langle R_h \rangle$ value can be pointed to the density distribution of the spherical particles. It is well-known that, for a uniform nondraining sphere, the ratio is 0.774. A higher $\langle R_g \rangle / \langle R_h \rangle$ value indicates a lower intensity in the core of the spherical particles. When $\langle R_g \rangle / \langle R_h \rangle = 1$, it can be attributed to a vesicle geometry in theory. In the current system, as shown in Table 2, the ratios of these samples are 1.02, 0.799, 0.818, and 0.866, respectively. The values indicate that the aggregate of ESLs are partially hollow in varying degrees. Among them, ESL-1 is more close to a typical vesicle structure. The results are in agreement with the microscope observations.

3.3. Self-Assembly Behavior of ESLs with DMF as Common Solvent. The initial common solvent is also a remarkable factor that influences the self-assembly behavior of amphiphilic copolymers. With DMF as the common solvent, aggregates generated by the ESLs are all spherical micelles as shown in Figure 5. The spheres do not have complex interior morphologies compared with the related micelles formed in the THF system. The diameters and PDIs of the spheres were further characterized by DLS. The $\langle R_h \rangle$ values of the samples are 107, 101, 58, and 70 nm, respectively, which agree well with the TEM observations. The ratios of the $\langle R_g \rangle$ to $\langle R_h \rangle$ are 0.791, 0.831, 0.855, and 0.829, respectively, for the four samples, which are close to the predicted value for a uniform sphere, 0.774.

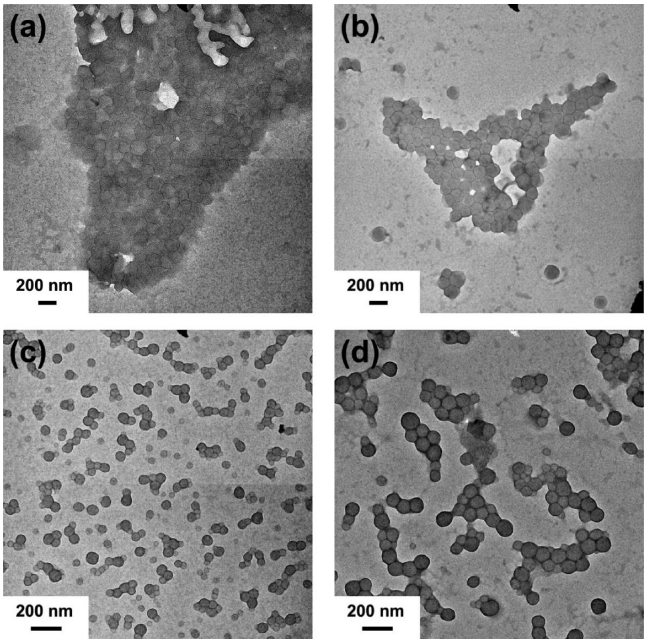

Figure 5. TEM photographs of the micelles formed by various ESL samples with DMF as initial solution: (a) ESL-1, (b) ESL-2, (c) ESL-3, and (d) ESL-4.

The formed aggregates are generally vesicles or large compound micelles in the THF system, while spherical micelles were prepared with DMF as initial solvent. The results suggest that the nature of the common solvent has a major effect on the aggregate morphology. The solubility parameter of DMF is 24.9 $(J/cm^3)^{1/2}$, which is much higher than that of THF [18.6 $(J/cm^3)^{1/2}$]. DMF is a poorer solvent for ESLs than THF because THF has a solubility parameter more close to PS and PCL blocks. It can be expected that the PS and PCL blocks in the copolymer chain are not stretched as extensively as in the THF system. Because the stretching is entropically unfavorable, if the degree of stretching is high, the stretch penalty for the PS and PCL blocks in the core would change the morphology from micelles to vesicles to decrease the overall free energy.[59] This could explain that the morphologies are primary spherical micelles with DMF as initial common solvent. In another aspect, the transition reveals that the property of solvent plays a crucial role in the microphase separation of copolymers because of the different chain mobilities in the solutions.

3.4. Proposed Mechanism of Multicompartment Micelles Formation. Summarizing all of the experimental findings, the mechanism of the formation of multicompartment micelles formed by a of PEG-*b*-PS-*b*-PCL triblock copolymers is proposed. The copolymers self-assemble into spherical micelles with DMF as initial common solvent, while forming various hollow multicomponent structures in the THF system. Shown in Figure 6 is a schematic illustration of ESL hollow structures formed under the self-assembly process. In the stock solution of ESL in the common solvent THF, the polymer chains extend freely (Figure 6a). When deionized water is introduced, the hydrophobic PS and PCL blocks tend to self-associate because of the gradually decrease of the solubility, and the aggregation takes place with the hydrophilic PEG blocks surrounding. It has been argued that the morphologies of self-assemblies are controlled by three factors for a force balance, stretching of the core-forming blocks in the core, the repulsive interaction among the corona chains, and the interfacial tension at the core−corona interface.[60] While it differs from the self-association of traditional diblock or triblock copolymers, the self-assembly process is no longer solely determined by the amphiphilic property. The incompatibility of hydrophobic blocks of PS and PCL, which leads to the phase separation of these two blocks, is a crucial factor influencing the self-assembly behavior.

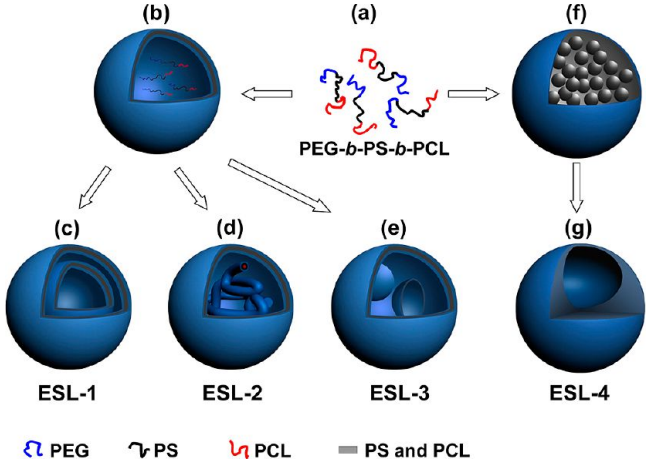

Figure 6. Schematic image showing the formation process of the hollow structures with THF as the initial solvent.

The formation kinetics of micelles from the unimer state is crucial for self-assembly research. In general, simple structures, such as spheres, rods, and vesicles, can be equilibrium

dx.doi.org/10.1021/jp312858e | J. Phys. Chem. B 2013, 117, 2586−2593

morphologies in a range of mixed solvents.[53] However, the compartmental structures are more likely to be formed via complicated process. In the present work, the ESL copolymers are more likely to form kinetically trapped structures. When a selective solvent, water, was added to the copolymer solution, the solubility of THF/H_2O mixed solvent to the PS and PCL blocks decreased gradually, and the copolymers self-associated together. When the water content is low, the copolymer chains have high mobility, and the free chain exchange in interaggregates and inner aggregates can be achieved. In this condition, the aggregates represent an equilibrium state. Because of the lower hydrophilic/hydrophobic ratios of the copolymers, these copolymers tend to self-assemble into vesicles or large compound micelles. More added water could freeze the copolymer chains to fix the overall morphologies. However, in such conditions, the volume fraction of THF is still relatively high in the inner part of the aggregates. Thus, copolymer chains in the inner aggregates still have certain mobility to form inner structures. After a large amount of water was added to system, the structures were frozen.

The ESLs have very low mobility in solution with the addition of water because of the high T_g PS blocks and semicrystalline PCL blocks. Therefore, in the micellization process, they are easy to form kinetically trapped structures. The ESL samples with a low hydrophilic/hydrophobic ratio prefer to form vesicles with many unimers entrapped in (Figure 6b). For ESL-1, the PCL blocks have similar chain lengths to the PS blocks and thus phase separation of lamellar structure within the aggregates is generated. So the multilamellar structures are formed (Figure 6c). With increasing PS blocks of ESL-2, PCL blocks tend to form the core surrounding by PS blocks. Hence, cylindrical structures are formed within the vesicles (Figure 6d). For ESL-3, entrapped vesicles are generated due to the copolymer unimers entrapped in formed vesicles further self-assemble into small vesicles (Figure 6e). If the ESL-4 copolymers with longer PS blocks self-assemble to vesicles, the dimension of the wall inner layer will be much larger than that of ESL-3 vesicles. The PEG block cannot protect the hydrophobic wall of the vesicle any more. Therefore, large compound micelles are formed to minimize the total energy of the system (Figure 6f). In the process, the solvents can be entrapped by the fast freezing shells of the aggregates, leading to formation of porous large compound micelles (Figure 6g).

From the results, we learned that compartmental micelles with varying hollow patterns can be prepared by tuning the component of block copolymers. The hollow patterns can endow the micelles with diverse properties for incorporating drugs or serving as templates. Because the PCL segment is biodegradable, the self-assembly behavior of the ESLs can be responsive to certain enzymes in biological systems, similar to other environmental responsive polymers.[61,62] Thus, the micelles possessing hollow spaces in nano size may be potential candidates for nanoreactors, nanocarriers, and the likes.

4. CONCLUSIONS

The self-assembly behaviors of PEO-*b*-PS-*b*-PCL copolymers in aqueous solution were investigated with TEM, SEM, and LLS. It revealed that these copolymers can self-assemble to complex vesicles and LCMs by tuning the component of the copolymers with THF as initial common solvent. With DMF as initial common solvent, the morphologies change to spherical micelles, indicating that the initial solvent is also a crucial factor influencing the self-assembly behavior. Summarizing the experimental results, the mechanism of the formation of the structure aggregates was suggested.

AUTHOR INFORMATION

Corresponding Author

*E-mail: xhhe@chem.ecnu.edu.cn (X.H.); jlin@ecust.edu.cn (J.L.). Tel.: +86-21-6425-3370. Fax: +86-21-6425-3539.

Notes

The authors declare no competing financial interest.

ACKNOWLEDGMENTS

This work was supported by National Natural Science Foundation of China (51103044, 21174038, and 50925308). Support from Projects of Shanghai Municipality (11QA1401600, 13ZZ041, and 12JC1403102) and Fundamental Research Funds for the Central Universities (20100074120001, NCET-12-0857, and WD1213002) is also appreciated.

REFERENCES

(1) Zhang, L.; Eisenberg, A. Multiple Morphologies of "Crew-Cut" Aggregates of Polystyrene-*b*-poly(acrylic acid) Block Copolymers. *Science* **1995**, *268*, 1728−1731.

(2) Yu, S.; Azzam, T.; Rouiller, I.; Eisenberg, A. Breathing Vesicles. *J. Am. Chem. Soc.* **2009**, *131*, 10557−10566.

(3) Lin, S.; He, X.; Li, Y.; Lin, J.; Nose, T. Brownian Molecular Dynamics Simulation on Self-Assembly Behavior of Diblock Copolymers: Influence of Chain Conformation. *J. Phys. Chem. B* **2009**, *113*, 13926−13934.

(4) Mai, Y.; Eisenberg, A. Self-assembly of Block Copolymers. *Chem. Soc. Rev.* **2012**, *41*, 5969−5985.

(5) Marinakos, S. M.; Anderson, M. F.; Ryan, J. A.; Martin, L. D.; Feldheim, D. L. Encapsulation, Permeability, and Cellular Uptake Characteristics of Hollow Nanometer-Sized Conductive Polymer Capsules. *J. Phys. Chem. B* **2001**, *105*, 8872−8876.

(6) Jaramillo, T. F.; Baeck, S. H.; Cuenya, B. R.; McFarland, E. W. Catalytic Activity of Supported Au Nanoparticles Deposited from Block Copolymer Micelles. *J. Am. Chem. Soc.* **2003**, *125*, 7148−7149.

(7) Sohn, B. H.; Choi, J. M.; Yoo, S. I.; Yun, S. H.; Zin, W. C.; Jung, J. C.; Kanehara, M.; Hirata, T.; Teranishi, T. Directed Self-Assembly of Two Kinds of Nanoparticles Utilizing Monolayer Films of Diblock Copolymer Micelles. *J. Am. Chem. Soc.* **2003**, *125*, 6368−6369.

(8) Savić, R.; Luo, L.; Eisenberg, A.; Maysinger, D. Micellar Nanocontainers Distribute to Defined Cytoplasmic Organelles. *Science* **2003**, *300*, 615−618.

(9) Lin, S.; Numasawa, N.; Nose, T.; Lin, J. Brownian Molecular Dynamics Simulation on Self-Assembly Behavior of Rod-coil Diblock Copolymers. *Macromolecules* **2007**, *40*, 1684−1692.

(10) Lin, J.; Zhu, J.; Chen, T.; Lin, S.; Cai, C.; Zhang, L.; Zhuang, Y.; Wang, X. S. Drug Releasing Behavior of Hybrid Micelles Containing Polypeptide Triblock Copolymer. *Biomaterials* **2009**, *30*, 108−117.

(11) Li, W.; Liu, S.; Deng, R.; Zhu, J. Encapsulation of Nanoparticles in Block Copolymer Micellar Aggregates by Directed Supramolecular Assembly. *Angew. Chem., Int. Ed.* **2011**, *50*, 5865−5868.

(12) Liu, Y.; Lor, C.; Fu, Q.; Pan, D.; Ding, L.; Liu, J.; Lu, J. Synthesis of Copper Nanocatalysts with Tunable Size Using Diblock Copolymer Solution Micelles. *J. Phys. Chem. C* **2010**, *114*, 5767−5772.

(13) Schappacher, M.; Deffieux, A. Synthesis of Macrocyclic Copolymer Brushes and Their Self-Assembly into Supramolecular Tubes. *Science* **2008**, *319*, 1512−1515.

(14) Schatz, C.; Louguet, S.; Le Meins, J. F.; Lecommandoux, S. Polysaccharide-block-polypeptide Copolymer Vesicles: Towards Synthetic Viral Capsids. *Angew. Chem., Int. Ed.* **2009**, *48*, 2572−2575.

(15) Wei, H.; Wu, D. Q.; Li, Q.; Chang, C.; Zhou, J. P.; Zhang, X. Z.; Zhuo, R. X. Preparation of Shell Cross-Linked Thermoresponsive

Micelles as well as Hollow Spheres Based on P(NIPAAm-co-HMAAm-co-MPMA)-*b*-PCL. *J. Phys. Chem. C* **2008**, *112*, 15329−15334.
(16) Meng, X. W.; Ha, W.; Cheng, C.; Dong, Z. Q.; Ding, L. S.; Li, B. J.; Zhang, S. Hollow Nanospheres Based on the Self-Assembly of Alginate-graft-poly(ethylene glycol) and α-Cyclodextrin. *Langmuir* **2011**, *27*, 14401−14407.
(17) Zhao, W.; Chen, D.; Hu, Y.; Grason, G. M.; Russell, T. P. ABC Triblock Copolymer Vesicles with Mesh-Like Morphology. *ACS Nano* **2011**, *5*, 486−492.
(18) Tao, Y.; Liu, X.; Shi, D.; Chen, M.; Yang, C.; Ni, Z. Graft-like Block Copolymer Bearing Biodegradable ε-Caprolactone Branches: A Facile Route to Hollow Nanocages. *J. Phys. Chem. C* **2009**, *113*, 6009−6013.
(19) Blanazs, A.; Armes, S. P.; Ryan, A. J. Self-Assembled Block Copolymer Aggregates: From Micelles to Vesicles and their Biological Applications. *Macromol. Rapid Commun.* **2009**, *30*, 267−277.
(20) Sumerlin, B. S.; Vogt, A. P. Macromolecular Engineering through Click Chemistry and Other Efficient Transformations. *Macromolecules* **2009**, *43*, 1−13.
(21) Skrabania, K.; Laschewsky, A.; Berlepsch, H. v.; Böttcher, C. Synthesis and Micellar Self-Assembly of Ternary Hydrophilic-Lipophilic-Fluorophilic Block Copolymers with a Linear PEO Chain. *Langmuir* **2009**, *25*, 7594−7601.
(22) Yang, S. K.; Ambade, A. V.; Weck, M. Supramolecular ABC Triblock Copolymers via One-Pot, Orthogonal Self-Assembly. *J. Am. Chem. Soc.* **2010**, *132*, 1637−1645.
(23) de Graaf, A. J.; Mastrobattista, E.; Vermonden, T.; van Nostrum, C. F.; Rijkers, D. T. S.; Liskamp, R. M. J.; Hennink, W. E. Thermosensitive Peptide-Hybrid ABC Block Copolymers Obtained by ATRP: Synthesis, Self-Assembly, and Enzymatic Degradation. *Macromolecules* **2012**, *45*, 842−851.
(24) Hadjichristidis, N.; Iatrou, H.; Pitsikalis, M.; Pispas, S.; Avgeropoulos, A. Linear and Non-Linear Triblock Terpolymers. Synthesis, Self-assembly in Selective Solvents and in Bulk. *Prog. Polym. Sci.* **2005**, *30*, 725−782.
(25) Gröschel, A. H.; Schacher, F. H.; Schmalz, H.; Borisov, O. V.; Zhulina, E. B.; Walther, A.; Müller, A. H. E. Precise Hierarchical Self-assembly of Multicompartment Micelles. *Nat. Commun.* **2012**, *3*, 710−720.
(26) Xu, L.; Zhang, Z.; Wang, F.; Xie, D.; Yang, S.; Wang, T.; Feng, L.; Chu, C. Synthesis, Characterization, and Self-assembly of Linear Poly(ethylene oxide)-block-poly(propylene oxide)-block-poly(ε-caprolactone) (PEO-PPO-PCL) Copolymers. *J. Colloid Interface Sci.* **2013**, *393*, 174−181.
(27) Qu, T.; Wang, A.; Yuan, J.; Gao, Q. Preparation of an Amphiphilic Triblock Copolymer with pH- and Thermo-responsiveness and Self-assembled Micelles Applied to Drug Release. *J. Colloid Interface Sci.* **2009**, *336*, 865−871.
(28) Li, Z.; Hillmyer, M. A.; Lodge, T. P. Morphologies of Multicompartment Micelles Formed by ABC Miktoarm Star Terpolymers. *Langmuir* **2006**, *22*, 9409−9417.
(29) Zhang, Y.; Liu, H.; Dong, H.; Li, C.; Liu, S. Micelles Possessing Mixed Cores and Thermoresponsive Shells Fabricated from Well-defined Amphiphilic ABC Miktoarm Star Terpolymers. *J. Polym. Sci., Polym. Chem.* **2009**, *47*, 1636−1650.
(30) Kubowicz, S.; Baussard, J. F.; Lutz, J. F.; Thünemann, A. F.; von Berlepsch, H.; Laschewsky, A. Multicompartment Micelles Formed by Self-Assembly of Linear ABC Triblock Copolymers in Aqueous Medium. *Angew. Chem., Int.* **2005**, *44*, 5262−5265.
(31) Moughton, A. O.; Hillmyer, M. A.; Lodge, T. P. Multicompartment Block Polymer Micelles. *Macromolecules* **2012**, *45*, 2−19.
(32) Wang, X.; Chen, J.; Hong, K.; Mays, J. W. Well-Defined Polyisoprene-*b*-Poly(acrylic acid)/Polystyrene-*b*-Polyisoprene-*b*-Poly(acrylic acid) Block Copolymers: Synthesis and Their Self-Assembled Hierarchical Structures in Aqueous Media. *ACS Macro Lett.* **2012**, *1*, 743−747.
(33) Zhou, Z.; Li, Z.; Ren, Y.; Hillmyer, M. A.; Lodge, T. P. Micellar Shape Change and Internal Segregation Induced by Chemical Modification of a Tryptych Block Copolymer Surfactant. *J. Am. Chem. Soc.* **2003**, *125*, 10182−10183.
(34) Uhrich, K. E.; Cannizzaro, S. M.; Langer, R. S.; Shakesheff, K. M. Polymeric Systems for Controlled Drug Release. *Chem. Rev.* **1999**, *99*, 3181−3198.
(35) Quan, C. Y.; Wu, D. Q.; Chang, C.; Zhang, G. B.; Cheng, S. X.; Zhang, X. Z.; Zhuo, R. X. Synthesis of Thermo-Sensitive Micellar Aggregates Self-Assembled from Biotinylated PNAS-*b*-PNIPAAm-*b*-PCL Triblock Copolymers for Tumor Targeting. *J. Phys. Chem. C* **2009**, *113*, 11262−11267.
(36) Shi, S.; Fan, M.; Wang, X.; Zhao, C.; Wang, Y.; Luo, F.; Zhao, X.; Qian, Z. Synthesis and Characterization of mPEG-PCL-*g*-PEI and Self-Assembled Nanoparticle Uptake in Vitro and in Vivo. *J. Phys. Chem. C* **2010**, *114*, 21315−21321.
(37) Huang, X.; Xiao, Y.; Lang, M. Self-assembly of pH-sensitive Mixed Micelles based on Linear and Star Copolymers for Drug Delivery. *J. Colloid Interface Sci.* **2011**, *364*, 92−99.
(38) Wang, T.; Li, M.; Gao, H.; Wu, Y. Nanoparticle Carriers based on Copolymers of Poly(ε-caprolactone) and Hyperbranched Polymers for Drug Delivery. *J. Colloid Interface Sci.* **2011**, *353*, 107−115.
(39) Lim Soo, P.; Eisenberg, A. Preparation of Block Copolymer Vesicles in Solution. *J. Polym. Sci. Part B: Polym. Phys.* **2004**, *42*, 923−938.
(40) He, X.; Zhang, H.; Wang, X. Synthesis of Side Chain Liquid Crystal-coil Diblock Copolymers with p-methoxyazobenzene Side Groups by Atom-transfer Radical Polymerization. *Polym. J.* **2002**, *34*, 523−528.
(41) He, X.; Liang, L.; Xie, M.; Zhang, Y.; Lin, S.; Yan, D. Synthesis of Novel Linear PEO-*b*-PS-*b*-PCL Triblock Copolymers by the Combination of ATRP, ROP, and a Click Reaction. *Macromol. Chem. Phys.* **2007**, *208*, 1797−1802.
(42) Floudas, G.; Reiter, G.; Lambert, O.; Dumas, P. Structure and Dynamics of Structure Formation in Model Triarm Star Block Copolymers of Polystyrene, Poly(ethylene oxide), and Poly(ε-caprolactone). *Macromolecules* **1998**, *31*, 7279−7290.
(43) Ma, M.; He, Z.; Yang, J.; Wang, Q.; Chen, F.; Wang, K.; Zhang, Q.; Deng, H.; Fu, Q. Vertical Phase Separation and Liquid-Liquid Dewetting of Thin PS/PCL Blend Films during Spin Coating. *Langmuir* **2011**, *27*, 1056−1063.
(44) Nojima, S.; Satoh, K.; Ashida, T. Morphology Formation by Combined Effect of Crystallization and Phase Separation in a Binary Blend of Poly(ε-caprolactone) and Polystyrene Oligomer. *Macromolecules* **1991**, *24*, 942−947.
(45) Chun, Y. S.; Kyung, Y. J.; Jung, H. C.; Kim, W. N. Thermal and Rheological Properties of Poly(ε-caprolactone) and Polystyrene Blends. *Polymer* **2000**, *41*, 8729−8733.
(46) Li, Y.; Stein, M.; Jungnickel, B. J. Competition between Crystallization and Phase Separation in Polymer Blends I. Diffusion Controlled Supermolecular Structures and Phase Morphologies in Poly(ε-caprolactone)/polystyrene Blends. *Colloid Polym. Sci.* **1991**, *269*, 772−780.
(47) Fu, J.; Cong, Y.; Li, J.; Luan, B.; Pan, C.; Yang, Y.; Li, B.; Han, Y. Hole Nucleation and Growth Induced by Crystallization and Microphase Separation of Thin Semicrystalline Diblock Copolymer Films. *Macromolecules* **2004**, *37*, 6918−6925.
(48) Zhang, F.; Chen, Y.; Huang, H.; Hu, Z.; He, T. Boundary Effect of Relief Structure on Crystallization of Diblock Copolymer in Thin Films. *Langmuir* **2003**, *19*, 5563−5566.
(49) Fu, J.; Wei, Y.; Xue, L.; Luan, B.; Pan, C.; Li, B.; Han, Y. Lamella Reorientation in Thin Films of a Symmetric Poly(l-lactic acid)-block-polystyrene upon Crystallization at Different Temperatures. *Polymer* **2009**, *50*, 1588−1595.
(50) Shen, H.; Eisenberg, A. Control of Architecture in Block-Copolymer Vesicles. *Angew. Chem., Int.* **2000**, *39*, 3310−3312.
(51) Peng, X.; Zhang, L. Formation and Morphologies of Novel Self-Assembled Micelles from Chitosan Derivatives. *Langmuir* **2007**, *23*, 10493−10498.

(52) Yu, K.; Eisenberg, A. Bilayer Morphologies of Self-Assembled Crew-Cut Aggregates of Amphiphilic PS-*b*-PEO Diblock Copolymers in Solution. *Macromolecules* **1998**, *31*, 3509−3518.
(53) Riegel, I. C.; Eisenberg, A.; Petzhold, C. L.; Samios, D. Novel Bowl-Shaped Morphology of Crew-Cut Aggregates from Amphiphilic Block Copolymers of Styrene and 5-(N,N-Diethylamino)isoprene. *Langmuir* **2002**, *18*, 3358−3363.
(54) Liu, X.; Kim, J. S.; Wu, J.; Eisenberg, A. Bowl-Shaped Aggregates from the Self-Assembly of an Amphiphilic Random Copolymer of Poly(styrene-co-methacrylic acid). *Macromolecules* **2005**, *38*, 6749−6751.
(55) Wang, J.; Kuang, M.; Duan, H.; Chen, D.; Jiang, M. pH-dependent Multiple Morphologies of Novel Aggregates of Carboxyl-terminated Polymide in Water. *Eur. Phys. J. E* **2004**, *15*, 211−215.
(56) Wu, C.; Li, M.; Kwan, S. C. M.; Liu, G. J. Laser Light Scattering Characterization of a Novel Polymer Nanofiber. *Macromolecules* **1998**, *31*, 7553−7554.
(57) Chu, B. *Laser Light Scattering—Basic Principles and Practice*, 2nd ed.; Academic Press: New York, 1991.
(58) Wang, Y.; Lin, S.; Zang, M.; Xing, Y.; He, X.; Lin, J.; Chen, T. Self-assembly and Photo-responsive Behavior of Novel ABC_2-type Block Copolymers Containing Azobenzene Moieties. *Soft Matter* **2012**, *8*, 3131−3138.
(59) Yu, Y.; Zhang, L.; Eisenberg, A. Morphogenic Effect of Solvent on Crew-Cut Aggregates of Apmphiphilic Diblock Copolymers. *Macromolecules* **1998**, *31*, 1144−1154.
(60) Shen, H.; Zhang, L.; Eisenberg, A. Multiple pH-Induced Morphological Changes in Aggregates of Polystyrene-block-poly(4-vinylpyridine) in DMF/H_2O Mixtures. *J. Am. Chem. Soc.* **1999**, *121*, 2728−2740.
(61) Yu, B.; Jiang, X.; Wang, R.; Yin, J. Multistimuli Responsive Polymer Nanoparticles on the basis of the Amphiphilic Azobenzene-Contained Hyperbranched Poly(ether amine) (hPEA-AZO). *Macromolecules* **2010**, *43*, 10457−10465.
(62) Zhu, X.; Fryd, M.; Tran, B. D.; Ilies, M. A.; Wayland, B. B. Modifying the Hydrophilic-Hydrophobic Interface of PEG-*b*-PBO-*b*-PCL to Increase Micelle Stability: Preparation of PEG-*b*-PBO-*b*-PCL Triblock Copolymers, Micelle Formation, and Hydrolysis Kinetics. *Macromolecules* **2012**, *45*, 660−665.